JOURNAL GEOLOGICAL SOCIETY OF INDIA
Vol.71, February 2008, pp.171-188

Trace Element Variations in Deccan Basalts: Roles of Mantle Melting, Fractional Crystallization and Crustal Assimilation

NILANJAN CHATTERJEE[1] and SOMDEV BHATTACHARJI[2]

[1]Department of Earth, Atmospheric and Planetary Sciences, Room 54-1216, Massachusetts Institute of Technology, Cambridge, Massachusetts 02139, USA

[2]Department of Geology, Brooklyn College and Graduate Center of the City University of New York, Brooklyn, New York 11210, USA

Abstract: The variation in incompatible trace element contents of lower basaltic dykes and flows from different parts of the Deccan province was assessed through modelling of partial melting of primitive mantle and fractional crystallization of the parental melts coupled with crustal assimilation (AFC). Variations in Ba/Zr, Rb/Y and Nb/Y can be attributed to different degrees of partial melting of mantle. Variations in Zr, rare earth elements and Rb/Nb indicate fractional crystallization and significant coupled crustal assimilation away from the Deccan plume center. The Zr variation near the plume center can be explained through only fractional crystallization without the involvement of crust. AFC modelling of available Sr-Nd isotope data requires very high and unreasonable amounts of crustal assimilant implying that the parental magmas may have acquired their isotopic characteristics before AFC occurred in crustal magma chambers. The occurrence of AFC away from the plume center in the Narmada-Tapti rift region may be related to longer and greater magma-wall rock interaction in shallow crustal magma chambers due to crustal extension-related enlargement of the magma chambers, recharge with fresh, hot magma and convective mixing.

Keywords: Deccan, Basalt, Trace element, Partial melting, Fractional crystallization, Crustal assimilation.

INTRODUCTION

Continental flood basalts are thought to have originated by melting of mantle plumes of primitive chemical composition (Morgan, 1972; Richards et al. 1989a,b; Campbell and Griffith, 1990; Duncan and Richards, 1991; Courtillot et al. 1999). Compositions of parental magmas depend on the source rock compositions and the process and the extent of mantle melting. The parental magmas, however, rarely reach the surface. Basalts erupted on the surface are mostly the differentiated products of the parental magmas whose compositions have been altered by crystal fractionation and crustal contamination through wall rock assimilation during passage through crust. Therefore, the chemical compositions of the parental magmas are mostly inferred through geochemical modelling.

Concentrations of incompatible trace elements in parental melts may be predicted through mantle melting models as a function of the degree of melting (Presnall, 1969; Shaw, 1970). Equilibrium batch melting and fractional melting are the two end-member models for mantle melting. In equilibrium batch melting, the melt is in equilibrium with the residual minerals until removed from the source. In fractional melting, melt is constantly removed from the source so that only the last drop of melt is in equilibrium with the residue. Partial melting usually happens in eutectic mineral proportions in the source. This type of partial melting is also known as non-modal melting. Vijaya Kumar (2006) has recently reviewed the different mechanisms of mantle melting. Both equilibrium and fractional melting result in an enrichment of the incompatible elements in the initial melt fractions. In equilibrium melting, the incompatible element composition of the fractionated melts approaches the source composition with increasing degree of melting. On the other hand, fractional melting efficiently produces depleted melts at high degrees of melting; the incompatible element contents of the depleted melts may be lower than those of the source.

Pressure, temperature and volatile content of the magma and wall rock, and dynamics in magma conduits and chambers are important factors that control wall rock assimilation. Higher magma temperature, wall rock with lower melting point and longer magma chamber residence facilitate assimilation. These conditions are commonly found in upper crustal magma chambers. On the other hand, wall

rock with higher melting point and shorter magma-wall rock interaction lessen assimilation. These conditions are likely to occur in lower crustal magma conduits and chambers near the plume center.

In recent years, great strides have been made in understanding contamination through Sr-Nd-Pb isotope systematics in the Deccan Traps of western India, one of the largest and well studied flood basalt provinces in the world (Mahoney et al. 1982, 1985, 2000; Cox and Hawkesworth, 1984; Lightfoot and Hawkesworth, 1988; Lightfoot et al. 1990, Peng et al. 1994, 1998; Peng and Mahoney, 1995; Chandrasekharam et al. 1999; Saha et al. 2001; Melluso et al. 2004, 2006; Bondre et al. 2006, etc.). A two-stage model of contamination, first by lower crust/ enriched upper mantle and then by upper crust, seems to explain the isotopic characteristics of most Deccan basalts (Peng et al. 1994). Although crustal assimilation is expected to accompany fractional crystallization because of energy constraints (assimilation-fractional crystallization, or AFC model of DePaolo, 1981), a lack of positive correlation between Ba/Zr and Zr in the Western Ghats formations led Hooper (1994) to argue against AFC. A decoupling of assimilation and fractional crystallization is also indicated in many parts of the Deccan by a positive correlation between differentiation indices that decrease with fractional crystallization (e.g. Mg/[Mg+Fe], or Mg#) and contamination indices that are expected to increase with assimilation (e.g. $^{87}Sr/^{86}Sr$). Such an anomaly prompted Cox and Hawkesworth (1985) and Huppert and Sparks (1985) to suggest a temperature-controlled assimilation mechanism. Cox and Hawkesworth (1985) and Devey and Cox (1987) argued that contamination largely occurred during ascent and before gabbroic fractionation.

Recent studies have indicated several upper crustal magma chambers in the western margin rift and the intra-plate Narmada-Tapti rift of the Deccan province through two- and three-dimensional gravity modelling (Kaila et al. 1985; Kaila, 1988; Kaila and Krishna, 1992; Bhattacharji et al. 2004; Chatterjee and Bhattacharji, 2001). These shallow crustal magma chambers at depths between 5 and 7 km (Bhattacharji et al. 1996) are the ideal sites for magma differentiation and crustal contamination before the eruption of the basalts. In this study, we assess the relative importance of mantle melting, fractional crystallization and crustal contamination through batch and fractional melting, and assimilation-fractional crystallization calculations to explain the incompatible trace element variations in the erupted basalts immediately above the shallow magma chambers. This study sheds light on the mechanism and physical-chemical conditions of crustal contamination through an evaluation of area-to-area variability in assimilant amounts in the Deccan province.

GEOLOGICAL BACKGROUND AND PREVIOUS WORK

The 68.6-63.8 Ma old Deccan Traps of western India (Duncan and Pyle, 1988; Courtillot et al. 1988; Venkatesan et al. 1993, Basu et al. 1993; Baksi, 1994; Bhattacharji et al. 1996; Allegre et al. 1999; Chatterjee and Bhattacharji, 2001) is one the largest continental flood basalt provinces in the world (Fig. 1). This province covers an area of more than $5x10^5$ km^2 with an estimated volume of $5.12x10^5$ km^3 (Courtillot et al. 1986) and has a thickness of almost 3.5 km in the Western Ghats region where high to low-angle rift faults parallel the Panvel flexure and the western coast of India. The E-W to ENE-WSW Narmada-Tapti mid-continental rift and the approximately N-S Cambay rift intersect the western margin rift near Surat forming a triple junction which coincides with a zone of gravity high that has been interpreted as the center of the Deccan plume-head (Burke and Dewey, 1973; Bose, 1980; Bhattacharji et al. 1996).

The Deccan flood basalt province presumably formed when the Indian plate was stationed over a hot spot (mantle plume) and subsequently drifted northward away from the hot spot (Morgan, 1972; Cox, 1983; Devey and Lightfoot, 1986; Mitchell and Widdowson, 1991). The hot spot was apparently responsible for the subsequent formation of the Chagos-Laccadive ridge and is currently manifest as the volcanism at Reunion Island (Morgan, 1972; Duncan and Pyle, 1988). White and McKenzie (1989) suggested a quantitative model for continental flood basalt volcanism due to elevated geothermal gradients of hot spots in association with continental rifting events, whilst Richards et al. (1989b) proposed a model involving rising diapirs which become trapped at the crust-mantle boundary thus feeding the surface eruptions through crustal lineaments and rifts, as shown by Bhattacharji et al. (1996) from field, geophysical and geochemical studies (Fig.2). When the Indian plate was stationary over the hot spot, vigorous convecting circulation induced homogenization in the anomalous mantle as seen in simulation model experiments (Fig.2; Bhattacharji and Koide, 1987, Plates 1 and 2, Fig. 8B). Partial melting occurred in this homogenized mantle to form the parental magmas of the Deccan basalts. When the Indian plate moved northward and passed over the hot spot different magma reservoirs formed at the western margin of India as indicated by gravity highs in the

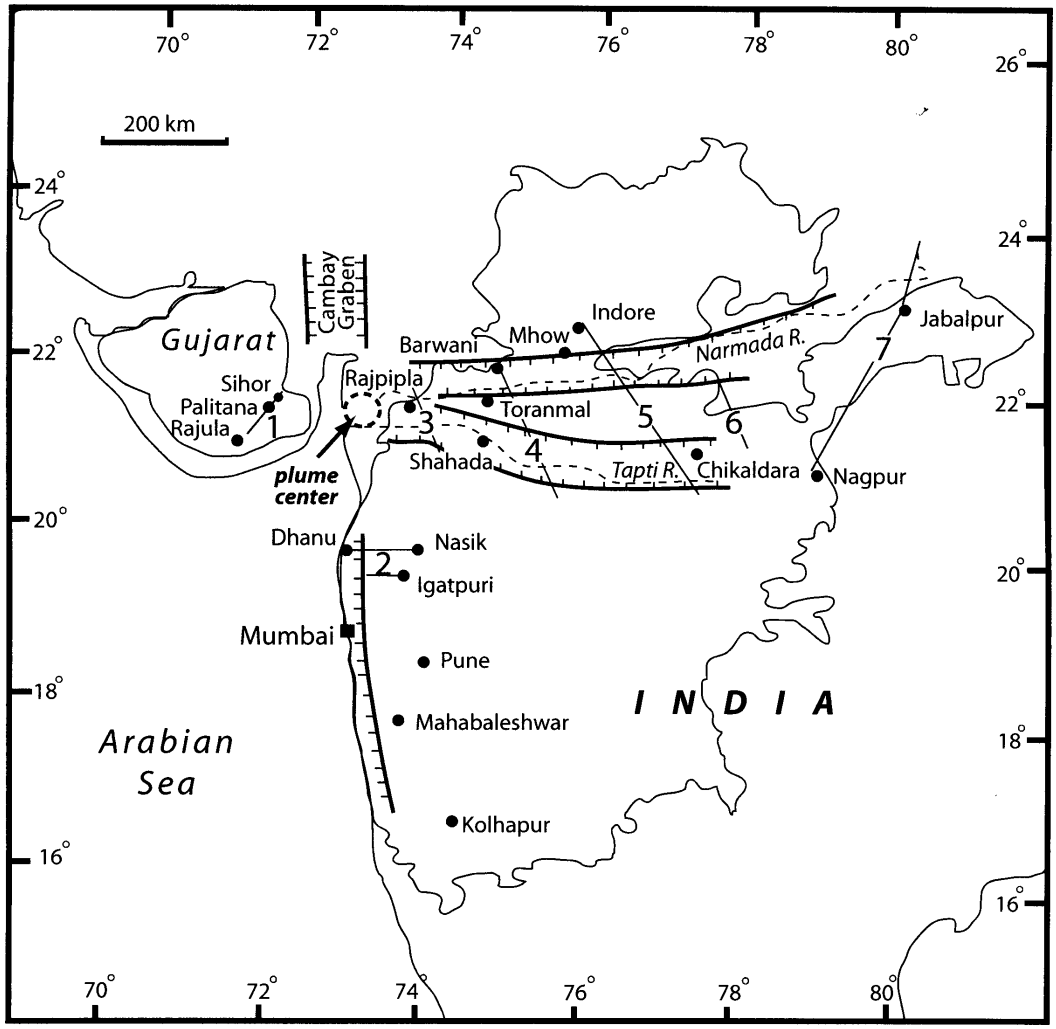

Fig.1. Map showing the extent of the Deccan flood basalt province on the Indian shield. Location of the studied areas, major cities and the major faults and rifts are also shown. The numbered lines indicate sample traverses and the circle in dashed line represents the position of the plume center (from Bhattacharji et al. 1996); 1 – Sihor-Palitana-Rajula, 2 – Igatpuri and Dhanu-Nasik, 3 – Amba Dongar, 4 – Barwani-Jalgaon, 5 – Indore-Khargaon, 6 – Betul-Salbardi, 7 – Panna-Nagpur.

Gujarat and Mumbai areas (Chatterjee and Bhattacharji, 2001; Bhattacharji et al. 2004).

Cox and Hawkesworth (1984), Beane et al. (1986), Subbarao and Hooper (1988) and Lightfoot et al. (1990) presented a detailed chemical stratigraphy of the Western Ghats section at the western continental margin of India. On the basis of their chemical data, the Deccan Basalts Group is classified into three subgroups. From bottom to top, they are the Kalsubai, Lonvala and Wai subgroups. The subgroups are further divided into formations. From bottom to top, the Kalsubai subgroup consists of the Igatpuri-Jawhar, Neral, Thakurvadi and Bhimshankar Formations, the Lonvala subgroup includes the Khandala and Bushe Formations and the Wai subgroup is made of the Poladpur, Ambenali, Mahabaleshwar and Panhala Formations. The extent of these formations in the other parts of the Deccan Province is uncertain. However, recent studies along the Narmada-Tapti rift have identified Ambenali-type basalts at Jabalpur in the far east of the province (Peng et al. 1998) and the Poladpur Formation possibly extends into the Toranmal area (Mahoney et al. 2000).

The first convincing evidence of crustal contamination of the Deccan parental magmas was presented by Mahoney et al. (1982), who concluded from Nd and Sr-isotope data that the basalts near Mahabaleshwar originated by mixing of an uncontaminated Ambenali-type parental magma with two different contaminants: upper continental crust (the Ambaneli-Poladpur trend) and an enriched mantle or lower crust (the Ambenali-Mahabaleshwar trend). Cox and Hawkesworth (1984) used mass balance calculations

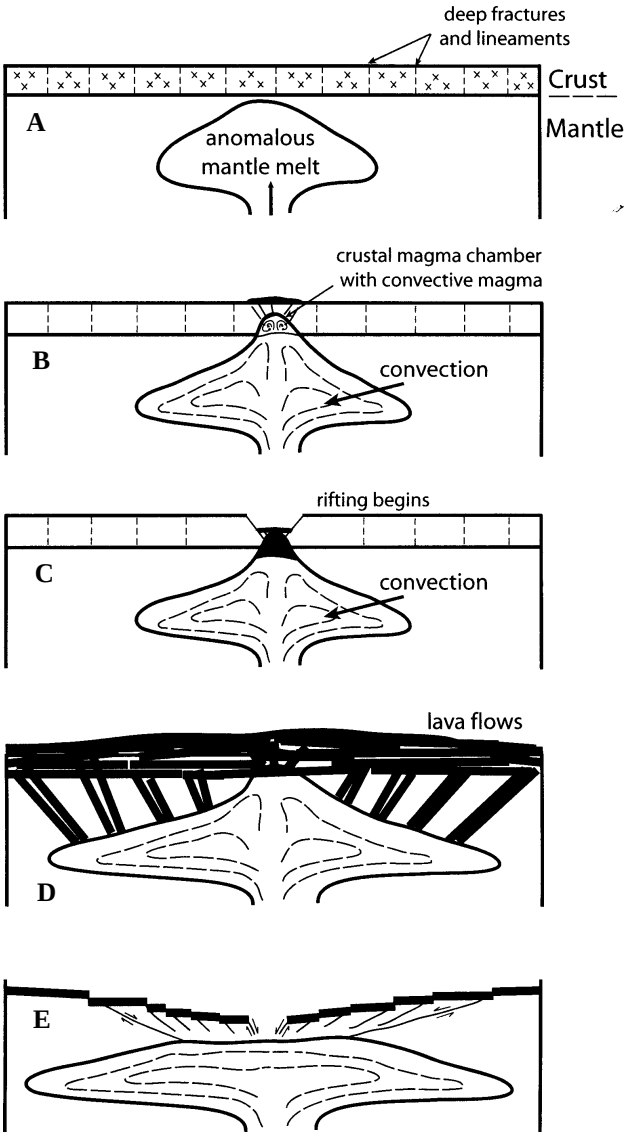

Fig.2. Diagrammatic representation of Deccan flood basalt evolution by convective (anomalous) mantle formed over the hot spot. (**A**) anomalous mantle melt (lower density melt due to melting of mantle material over the hot spot or plume) rises to the base of the crust that contains deep faults and lineaments; (**B**) vigorously circulating mantle melt pierces crust through the preexisting deep faults and lineaments; (**C**) conical magma chamber forms and lithospheric rifting begins; (**D**) magma erupts through several vents simultaneously and forms voluminous lava flows; (**E**) lithosphere rifts laterally in active response to the flood basalt eruption and forms rift valleys.

to estimate that the Poladpur Formation basalts originated by 6-12 wt% mixing of a granitic component with Ambenali-type basalts. Isotopic evidence further indicates that granitic contamination is widespread in the Bushe Formation, the most contaminated of the Deccan basalts (Cox and Hawkesworth, 1984), and Mahabaleshwar-type contamination is also present in the Panhala Formation (Lightfoot and Hawkesworth, 1988; Lightfoot et al. 1990). However, Peng et al. (1994) showed that the Ambenali-Poladpur trend is absent in Nd-Pb isotope diagrams, in which the Poladpur and Bushe lavas plot in separate fields seemingly unrelated to Ambenali. Peng et al. (1994) used Sr, Nd, Pb and O-isotope data to present a two-stage contamination model for the Lonvala and Kalsubai subgroup basalts, a lower crustal contamination resulting in intermediate "common signature" (CS) basalts that further interacted with various types of continental granulites to generate the basalts of the lower and middle subgroup formations. Hf-Nd isotopes from the Western Ghats (Saha et al. 2001) and Sr-Nd isotopes from the Sangamner dike swarm, east of the Western Ghats (Bondre et al. 2006) are also consistent with the two-stage model. However, the CS members of the two-stage model are yet to be recognized in the Western Ghats.

Along the Narmada-Tapti rift, lavas sampled at Rajpipla, Toranmal, Shahada-Nandarde, Mhow, Chikaladara and Jabalpur show a contamination trend similar to the Ambenali-Poladpur trend in a Sr-Nd isotope diagram (Mahoney et al. 1985, 2000; Peng et al. 1998; Chandrasekharam et al. 1999). However, Nd-Pb isotope plots indicate that some Jabalpur basalts went through only the first stage of contamination and hence possibly represent the intermediate members so far undetected in the Western Ghats. On the other hand, many of the Mhow, Chikaladara and Toranmal samples seem to have been contaminated through the second stage (Peng et al. 1998; Mahoney et al. 2000).

Samples from the Gujarat area also plot in the Ambenali and Poladpur fields in Sr-Nd-Pb isotope diagrams, but define tight arrays emanating from the fields of the Ambenali and Reunion lavas (Peng and Mahoney, 1995). These trends and some recent isotope data have been interpreted by Melluso et al. (2006) as resulting from mixing of the parental magmas with continental crust or mantle enriched with ancient subducted sediment.

The upward decrease in both Mg# and $^{87}Sr/^{86}Sr$ in the Poladpur-Ambenali part of the Western Ghats section indicate that contamination and fractional crystallization were independent processes (Cox and Hawkesworth, 1985). A rough overall negative correlation between $\varepsilon_{Nd}(t)$ and Mg# in the Toranmal section may also indicate a decoupling of fractional crystallization and contamination (Mahoney et al. 2000). Such decoupling relations, however, have not been recognized in the lower formations of Western Ghats (Beane et al. 1986).

METHODS

Our trace element models are based on chemical data on lower Deccan flows and dikes from five areas of the Deccan province encompassing Gujarat, the western continental margin and the mid-plate Narmada-Tapti rift (Fig. 1). The five areas are (1) Sihor-Palitana-Rajula (traverse 1, west of the Cambay rift in Gujarat), (2) Igatpuri and Dhanu-Nasik (traverse 2, Western Ghats areas near the presumed plume center), (3) Barwani-Jalgaon-Toranmal (traverse 4), (4) Indore-Mhow-Khargaon-Betul-Salbardi-Chikladara (traverses 5 and 6), and (5) Panna-Jabalpur-Seoni-Nagpur area (traverse 7). Area 5 is at the northeastern edge, and areas 3 and 4 are in the middle part of the Narmada-Tapti rift (Fig. 1). The compositional data are given in Table 1. The data are plotted in a SiO_2 versus total alkali discrimination diagram (Fig. 3a) and the average primitive mantle-normalized trace element concentrations for the five areas are shown in Fig. 3b. We have also used geochemical and isotope data from Mahoney et al. (1982, 1985, 2000), Cox and Hawkesworth (1985), Beane et al. (1986), Lightfoot and Hawkesworth (1988), Lightfoot et al. (1990), Peng et al. (1994, 1998), Peng and Mahoney (1995), Chandrasekharam et al. (1999) and Sheth et al. (2004) for the purpose of modeling.

The non-modal batch (equilibrium) and fractional melting equations (Presnall, 1969; Shaw, 1970) were used to model partial melting of primitive mantle (McDonough and Sun, 1995). These equations are:

$$C^l/C^0 = 1 / [\, D^0 + F(1 - P)\,] \quad (1)$$

and

$$C^l/C^0 = (1/D^0)\,(1 - FP/D^0)^{(1/P - 1)} \quad (2)$$

for non-modal batch (equilibrium) and fractional melting, respectively. In the above equations, C^l is the concentration of the trace element in the melt, C^0 the initial concentration in the source, D^0 the initial bulk solid/liquid partition coefficient, P the solid/liquid partition coefficient weighted to the melting proportions of the minerals, and F the fraction of melt. The mineral/liquid partition coefficients and the melting proportion of minerals are from Vijaya Kumar (2006).

We have used the general equations of assimilation-fractional crystallization (AFC) from DePaolo (1981) in our modeling. For trace elements and isotope ratios, these equations are:

$$\frac{C_m}{C_m^0} = F^{-z} + \left(\frac{a}{a-1}\right)\frac{C_a}{zC_m^0}\ln(1 - F^{-z}) \quad (3)$$

and

$$\varepsilon_m = \frac{\left(\frac{a}{a-1}\right)\frac{C_a}{z}(1 - F^{-z})\varepsilon_a + C_m^0 F^{-z}\varepsilon_m^0}{\left(\frac{a}{a-1}\right)\frac{C_a}{z}(1 - F^{-z}) + C_m^0 F^{-z}} \quad (4)$$

where, C is the concentration of the trace element, ε is the corresponding isotope ratio (e.g. $^{87}Sr/^{86}Sr$ and ε_{Nd}), subscripts $_m$ and $_a$ are for magma and assimilant, superscript ^{0} is for the original concentration in the magma, F is the fraction of magma remaining, a is the ratio of the rate of change of magma mass due to assimilation to the rate of change of magma mass due to fractional crystallization, and $z = (a+D-1)/(a-1)$ with D as the bulk solid/liquid partition coefficient for the element under consideration.

Crystal/basaltic liquid partition coefficients for incompatible elements are from the tabulations of Bedard (2001). Bulk solid/liquid partition coefficients were calculated using the experimentally determined modes of crystallizing phases from Sano et al. (2001). Since Sano et al. (2001) found different phase proportions using the QFM and NNO buffers and using uncontaminated and contaminated Deccan basalts as starting material in their melting experiments, the average of the phase proportions from their QFM and NNO experiments were used and the appropriate interpolations were made for contaminations in our models, wherever necessary. We used the least contaminated sample (lowest Zr and Rb/Y) as the starting composition and used the most contaminated sample (highest Zr and Rb/Y) as assimilant in each area in our calculations. In our models, crystallization was extended up to 64%, which is close to the average 67% average crystallization range recorded in Sano et al's (2001) experiments.

RESULTS

With a few exceptions the basalts in this study are tholeiites as shown in a SiO_2 versus total alkali plot (Fig.3a). The primitive mantle-normalized incompatible element patterns (Fig. 3b) show large-ion-lithophile element (LILE) enrichment over high-field-strength element (HFSE) and rare earth element (REE), Th peak, Sr trough, Nb depletion with respect to La, and a smoothly decreasing REE profile. The Palitana (Gujarat) samples especially show Nb-Ta and Ti troughs. The average La/Nb ratio of the Palitana samples (2.3) is higher than in the samples from the Narmada-Tapti rift (1.3) and the western continental margin (1.2). The average Nb/Ta ratio of the Palitana samples (12.1) is also lower than of the Narmada-Tapti samples (16.7, Toranmal, Mahoney et al. 2000). The higher La/Nb and lower Nb/Ta ratios may reflect a slightly different source

Table 1. Chemical composition of lower Deccan flows and dykes

	Dhanu-Nasik-Igatpuri														
	WTD-17 dyke	WTD-18 dyke	WTD-25 dyke	WTD-26 dyke	WTD-28 dyke	WTD-31 dyke	WTD-37 dyke	WTD-40 dyke	WTD-46 dyke	WTD-48 dyke	WPD-10 picrite dyke	WTF-4 flow	WTF-11 flow	WTF-13 flow	WTF-16 flow	WTF-17 flow
SiO_2	48.84	48.67	49.15	50.62	49.82	49.78	51.06	48.37	49.82	50.97	46.9	48.57	48.75	50.92	48.15	48.67
TiO_2	2.37	2.42	1.72	2.06	2.08	1.82	1.25	1.97	1.45	1.35	1.18	2.65	3.04	2.11	2.66	2.75
Al_2O_3	12.46	13.91	13.58	14.21	13.11	13.17	14.16	15.57	14.86	14.03	11	13.83	13.21	14.48	13.41	13.53
Fe_2O_3	16.57	15.76	12.03	14.08	15.18	12.69	13.05	12.74	12.33	13.78	12.81	14.21	15.61	13.56	15.17	15.41
MnO	0.22	0.2	0.16	0.17	0.2	0.17	0.19	0.17	0.19	0.2	0.17	0.17	0.2	0.17	0.22	0.22
MgO	5.23	5.65	7.25	5.16	5.83	7.88	6.16	6.49	6.5	5.69	15.91	5.5	4.83	4.91	5.41	5.55
CaO	10.08	10	11.64	9.96	10.1	11.21	10.3	11.16	11.03	9.83	8.75	10.41	9.08	9.73	10.23	10.25
Na_2O	2.45	2.5	1.92	2.29	2.41	1.87	2.37	2.4	2.2	2.5	1.54	2.54	2.62	2.66	2.41	2.5
K_2O	0.43	0.5	0.15	0.6	0.32	0.48	0.56	0.3	0.4	0.52	0.52	0.44	0.6	0.6.3	0.26	0.29
P_2O_5	0.25	0.29	0.2	0.22	0.24	0.22	0.2	0.27	0.2	0.22	0.16	0.3	0.4	0.26	0.29	0.3
LOI	0.82	-0.16	1.94	0.38	0.43	0.4	0.54	0.36	0.51	0.73	0.87	1.11	1.39	0.38	1.57	0.85
Total	99.82	99.74	99.74	99.75	99.75	99.69	99.84	99.8	99.49	99.82	99.81	99.73	99.73	99.81	99.78	100.32
Fe_2O_3*	2.49	2.36	1.80	2.11	2.28	1.90	1.96	1.91	1.85	2.07	1.92	2.13	2.34	2.03	2.28	2.31
FeO*	12.67	12.05	9.20	10.77	11.61	9.71	9.98	9.74	9.43	10.54	9.80	10.87	11.94	10.37	11.60	11.79
Mg#	42.38	45.52	58.41	46.07	47.23	59.14	52.38	54.28	55.13	49.04	74.32	47.43	41.90	45.77	45.39	45.63
Rb	12	16	10	19	11	15	23	14	16	17	19	13	27	23	12	11
Ba	73	66	76	134	79	101	108	60	65	126	105	143	217	185	65	82
Th	5	11	9	7	6	9	5	7	7	7	24	7	8	8	9	48
Nb	9	12	9	9	8	9	8	11	8	13	23	23	21	10	11	15
Ta																
Sr	198	226	285	272	206	239	130	221	154	147	154	296	242	255	237	240
Hf																
Zr	144	145	101	139	130	109	93	107	82	95	84	173	230	159	152	158
Y	32.73	32.23	21.19	27.86	31.69	23.1	30.5	24.97	26.42	28.48	18.82	31.87	39.64	31.33	33.16	34.12
La	11.97	11.79	12.43	14.94	11.66	12.24	13.4	10.16	8.56	13.66	10.77	21.02	26.05	19.8	13.16	12.83
Ce	28.56	27.95	26.23	32.74	27.16	27.52	27.84	23.02	19.5	29.04	22.32	46.11	55.19	41.27	30.67	29.49
Pr																
Nd	19.67	19.52	15.63	18.66	17.75	16.45	14.44	15.52	11.86	14.86	12.89	26.45	31.38	23.41	20.62	21.18
Sm	6.16	6.12	4.67	5.51	5.66	4.89	5.06	5.02	4.14	4.82	4.03	7.33	8.5	6.56	6.22	6.34
Eu	1.94	2.05	1.49	1.75	1.85	1.59	1.36	1.66	1.32	1.36	1.24	2.24	2.41	2.01	2.07	2.13
Gd	6.3	6.4	4.63	5.39	5.96	4.86	5.58	5.52	4.5	4.96	4.29	7.19	8.1	6.59	6.41	6.31
Tb																
Dy	6.27	6.15	3.75	4.98	5.84	4.17	5.32	4.82	4.66	5.02	3.36	6	7.47	5.9	6.22	6.39
Ho																
Er	2.81	2.75	1.74	2.31	2.75	1.93	3.28	2.48	2.36	2.98	1.63	2.84	3.33	2.68	2.83	2.82
Tm																
Yb	2.81	2.65	1.64	2.24	2.7	1.78	3.22	2.22	2.38	3.04	1.54	2.6	3.2	2.57	2.73	2.77
Lu	0.39	0.46	0.29	0.37	0.46	0.3	0.6	0.36	0.44	0.56	0.28	0.45	0.55	0.44	0.47	0.46
Be	1.6	1.79	1.29	1.7	1.7	1.5	1.2	1.6	1.38	1	1.1	1.79	2	1.7	1.79	1.88
Sc	36.5	34.7	36	32.5	37.7	34.5	39.9	33.5	36.2	38.9	28.78	34	31.78	32	35.7	36.59
V	475	475	329	345	396	312	339	340	319	339	339	361	388	337	456	493
Cr	45	90	372	81	104	560	136	192	224	58	2110	86	81	65	94	106
Co	45	50	48	44	43	49	44	41	44	43	177	39	40	43	47	46
Ni	50	88	141	68	72	147	69	107	106	50	774	78	71	64	82	88
Cu	188	283	165	175	240	168	177	187	165	175	77	264	358	192	276	283
Zn	115	115	84	102	107	92	88	95	82	99	83	105	124	105	119	126
Ga	16	37	24	27	23	25	20	29	26	28	120	30	33	28	31	39

Note: Oxides are in weight percent. Elements in ppm; the Th data are the maximum possible values (except in Gujarat samples); Mg# = Mg/(Mg+Fe); *Fe_2O_3 calculated assuming 15% of total Fe as in ferric state

Table 1. *Contd...*

	Amba Dongar					Palitana							Rajula-Sihor				
	WNTF-1 flow	WNTF-2 picrite flow	WNTF-3 flow	WNTF-4 flow	WNTF-5 flow	GF-1 flow	GF-2 flow	GF-3 flow	GF-4 flow	GF-5 flow	GF-6 flow	GF-7 flow	R-VI-2 dyke	CH-11 dyke	SH-4 dyke	SH-11 flow	SH-A-1 flow
SiO_2	46.51	46.47	48.96	45.77	48.01	48.39	49.41	48.53	51.58	50.7	50.44	48.73	51.78	46.45	46.83	49.84	50.11
TiO_2	3.4	1.18	1.22	1.18	2.06	1.16	1.09	1.98	1.73	1.62	1.09	2.23	1.18	2.02	1.25	1.51	1.17
Al_2O_3	13.17	10.19	14.71	13.23	13.51	16.37	16.17	15.45	14.19	14.4	14.98	13.22	14.63	13.61	14.45	13.85	14.32
Fe_2O_3	15.23	11.53	12.91	11.44	13.31	10.6	10.59	11.4	11.02	11.28	10.66	13.51	10.48	16.54	10.68	12.54	12.92
MnO	0.22	0.2	0.17	0.17	0.17	0.14	0.15	0.14	0.15	0.14	0.14	0.17	0.13	0.25	0.16	0.14	0.2
MgO	4.87	18.6	6.81	5.5	6.25	5.35	5.75	4.11	4.83	5.55	5.34	6.35	4.73	5.09	4.86	5.85	6.43
CaO	9.8	10.21	12.35	13.16	11.24	10.67	10.71	10.88	9.13	9.41	10.26	9.07	8.78	9.92	11.46	9.91	11.39
Na_2O	2.54	1.02	1.87	1.48	1.77	2.29	2.2	1.35	2.76	2.69	2.09	2.69	2.22	3.07	0.69	2.03	2.25
K_2O	0.86	0.3	0.28	0.05	0.6	0.29	0.28	0.02	1.09	0.71	0.68	0.63	1.45	0.78	0.09	0.94	0.34
P_2O_5	0.44	0.22	0.22	0.24	0.32	0.18	0.18	0.27	0.25	0.27	0.2	0.29	0.16	0.38	0.23	0.25	0.21
LOI	1.59	0.17	0.29	6.99	2.59	4.37	3.32	5.69	3.12	3.15	4	2.88	3.96	1.7	9.15	2.92	0.47
Total	98.63	100.09	99.79	99.21	99.83	99.81	99.85	99.82	99.85	99.92	99.88	99.77	99.5	99.81	99.85	99.78	99.81
Fe_2O_3*	2.28	1.73	1.94	1.72	2.00	1.59	1.59	1.71	1.65	1.69	1.60	2.03	1.57	2.48	1.60	1.88	1.94
FeO*	11.65	8.82	9.87	8.75	10.18	8.11	8.10	8.72	8.43	8.63	8.15	10.33	8.02	12.65	8.17	9.59	9.88
Mg#	42.70	78.99	55.15	52.84	52.25	54.05	55.86	45.66	50.53	53.42	53.86	52.28	51.26	41.77	51.47	52.09	53.70
Rb	22	15	11	5	21	8.68	8.87	8.45	31.8	19.6	20.9	17.2	43	29	3.91	47.96	9.62
Ba	197	101	46	27	146	164	102	17.4	226	175	206	191	309	294	25	121	100
Th	5	5	5	5	5	1	2.52	4.58	4.43	3.41	3.71	3.66	6		4.87	6.08	1.71
Nb	31	11	5	7	18	3.36	4.18	11.1	6.96	8.11	5.76	12.5	8	18	10.08	12.02	8.1
Ta						0.26	0.36	1.04	0.56	0.64	0.47	0.99					
Sr	389	270	158	175	359	306	214	337	261	365	248	324	126	221	129	274	151
Hf						1.97	2.29	4.1	3.82	3.62	3.03	4.17					
Zr	210	56	57	45	132	72.1	84.6	153	147	140	117	164	123	121	123	147	85
Y	36	12	22	20	28	21.1	21.3	26.9	24.3	22.4	25	28.1	23.475	38.76	26.4	28.6	25.4
La	26.49	11.91	7.2	7.7	17.6	7.59	10.98	18.41	18.39	20.14	15.92	19.82	19.93	16.42	51.61	62.1	31.76
Ce	63.95	35.12	24.08	22.74	45.14	16.45	23.32	39.57	39.96	43.2	32.13	43.1	141.85	59.94	40.32	48.39	24.73
Pr						2.21	2.92	4.97	4.97	5.41	3.86	5.54					
Nd	31.38	13.11	9.98	9.67	21.83	10.36	12.72	21.56	21.15	22.53	16.47	24.82	22.36	20.08	27.62	33.49	17.6
Sm	7.43	3.47	3.15	2.87	5.52	2.8	3.19	5.35	4.98	4.8	3.91	5.76	5.25	5.68	21.23	23.79	15.32
Eu	2.43	1.03	1.13	1.02	1.79	1.15	1.05	1.71	1.52	1.55	1.2	1.81	1.54	1.9	15.97	19.22	15.06
Gd	6.76	3.59	3.6	3.13	5.19	3.18	3.34	5.05	4.83	4.71	3.9	5.62	7.43	6.9	15.25	17.93	14.2
Tb						0.53	0.55	0.83	0.77	0.72	0.67	0.91			13.74	16.4	12.64
Dy	5.65	2.18	3.46	3.08	4.42	3.49	3.66	5.13	4.52	4.22	4.25	5.1	4.7	7.08	12.19	14.43	11.37
Ho						0.81	0.85	1.1	0.96	0.87	0.93	1.08					
Er	2.86	1.14	1.98	1.98	2.46	1.99	2.04	2.54	2.14	1.98	2.24	2.49	2.8	4.46	11.2	13.4	11.6
Tm						0.32	0.32	0.37	0.32	0.29	0.36	0.37			10.4	12.1	12.6
Yb	2.44	0.93	1.85	1.7	2.06	2.1	1.97	2.3	1.9	1.84	2.23	2.3	2.31	3.91	9.95	11.23	14.4
Lu	0.38	0.16	0.28	0.25	0.3	0.3	0.3	0.36	0.31	0.28	0.35	0.36	0.53	0.69			
Be						0.36	0.61	0.69	0.98	0.66	0.74	0.74	1.1	2	0.74	0.83	0.41
Sc						24.5	23.5	21.1	20.1	20	21.3	22	28	33.2			
V						265	244	298	302	283	255	329	250	430	269	309	131
Cr						167	121	173	118	125	104	283	134	48	46.6	25.8	120
Co						36.9	37.1	33.4	32.8	37.4	37.9	43.4	38	45	34	40	45.1
Ni	30	419	73	59	118	74.4	75.4	66.4	40	51.5	74.6	95.6	82	55	77	55.2	64.9
Cu	237	41	147	154	137	104	98.5	41.7	9.88	48.3	85.5	159	89	155	102	129	153
Zn	120	75	81	77	89	80.6	76.4	97.8	93.2	91.4	85.5	112	77	118	72.1	82.3	80.5
Ga						18.8	19.3	28.9	23.9	21.9	20.9	23.3	36	40	26.1	19.8	16.5

Note: Oxides are in weight percent. Elements in ppm; the Th data are the maximum possible values (except in Gujarat samples); Mg# = Mg/(Mg+Fe); *Fe_2O_3 calculated assuming 15% of total Fe as in ferric state

Table 1. *Contd...*

	Barwani-Jalgaon					Indore-Khargaon										Betul-Salbardi	
	6DN dyke	8.DT dyke	9.DTa dyke	DRKN-78 dyke	TFb flow	4.D1 dyke	5.D1a dyke	12.D1b dyke	13.D1b/FO dyke-flow	1.FB flow	2.F1 flow	3.F2 flow	10.FO flow	11.FOa flow	14.F flow	SAD-2 dyke	15.DTb/FO dyke-flow
SiO_2	51.31	51.91	47.23	66.81	50.12	51.01	50.01	49.87	49.47	50.36	51.12	50.21	49.07	48.37	46.67	47.73	48.23
TiO_2	2.79	0.9	3.84	0.7	2.02	2.17	2.58	2.88	2.33	2.68	3.53	3.04	2.41	3.44	1.26	1.83	2.25
Al_2O_3	12.68	15.08	12.96	9.78	13.51	13.49	12.58	12.63	13.23	13.58	13.31	14.78	13.07	14.53	14.41	14.05	13.38
Fe_2O_3	16.21	11.25	16.53	5.24	14.48	15.59	16.5	15.78	14.48	13.25	13.58	14.36	14.66	15.51	12.83	13.41	14.55
MnO	0.19	0.17	0.2	0.05	0.2	0.21	0.22	0.2	0.19	0.14	0.24	0.19	0.17	0.2	0.19	0.17	0.2
MgO	4.4	5.97	5.32	1.36	4.41	4.84	5.21	4.9	4.91	5.8	3.79	4.24	4.55	4.27	5.9	6.91	5.5
CaO	9.75	11.42	9.96	5.26	10.25	10.38	10.29	9.71	9.66	10.26	9.61	10.21	9.25	9.94	11.49	11.55	10.64
Na_2O	2.14	1.59	2.42	0.13	2.45	1.9	2.1	2.47	2.25	1.85	2.35	2.58	2.15	2.7	2.16	2.04	2.29
K_2O	0.97	0.63	0.51	5.48	0.36	0.45	0.38	0.5	0.91	0.84	1.45	0.86	0.64	0.53	0.14	0.11	0.4
P_2O_5	0.29	0.11	0.45	0.29	0.32	0.24	0.22	0.4	0.36	0.28	0.39	0.3	0.36	0.48	0.27	0.29	0.32
LOI				4.57													
Total	100.73	99.03	99.42	99.67	99.12	100.28	100.09	99.34	97.79	99.04	99.37	100.77	96.33	99.97	97.32	98.09	97.76
Fe_2O_3*	2.43	1.69	2.48	0.79	2.17	2.34	2.48	2.37	2.17	1.99	2.04	2.15	2.20	2.33	1.92	2.01	2.18
FeO*	12.40	8.60	12.64	4.01	11.07	11.92	12.62	12.07	11.07	10.13	10.39	10.98	11.21	11.86	9.81	10.26	11.13
Mg#	38.75	55.29	42.86	37.69	46.55	41.98	42.39	41.99	44.14	50.50	39.41	40.76	41.97	39.09	51.73	54.57	46.84
Rb	22	11	16	125	14	21	24	15	24	20	42	9	13	15	8	10	13
Ba	220	204	106	403	107	131	118	120	223	223	342	243	270	116	87	88	323
Th			5	5	5			5	5				5	5	5	5	5
Nb	13	7	20	5	11	10	10	16	13	21	32	23	13	22	8	9	10
Ta																	
Sr	273	175	246	1274	211	176	211	219	257	302	361	377	221	269	146	224	207
Hf																	
Zr	192	78	208	85	121	141	167	196	162	183	277	190	155	210	80	87	110
Y	35	23	41	18	32	36	38	42	35	32	43	31	33	42	30	24	30
La	29.09	20.95	18.26	16.11	14.64	22.6	16.91	20.24	19.9	20.96	43.71	27.92	19.48	17.85	12.4	7.77	10.55
Ce	50.36	39.25	50.23	33.38	36.65	31.69	34.25	51.68	50.18	47.19	78.5	5095	44.98	47.67	28.37	24.97	34.73
Pr																	
Nd	29.9	31.2	27.08	25.44	18.51	10.1		27.18	24.31	8.98	42.42	28.12	22.28	27.03	13.11	13.33	18.11
Sm	7.74	8.75	7.49	3.52	5.19	6.51	6.09	7.49	6.5	4.29	9.57	6.7	5.98	7.44	3.75	4.07	5.58
Eu	1.99	2.11	2.39	1.06	1.77	1.23	1.82	2.31	2.08	1.67	2.47	1.85	1.93	2.42	1.23	1.45	2.01
Gd			6.97	3.28	5.17			7.42	6.07				5.17	7.17	4.3	4.5	6.11
Tb	1.94	1.52				0.95	1.13			0.93	1.89	0.83					
Dy			6.56	3	5.12			7.03	5.73				4.95	6.32	4.65	4.06	5.35
Ho																	
Er			3.34	2.12	2.7			3.55	3.09				2.7	3.27	2.77	2.14	2.82
Tm																	
Yb	3.19	4.28	3.02	1.8	2.59	2.52	3.54	3.35	2.7	3.05	3.9	2.84	2.33	2.98	2.75	1.87	2.54
Lu	0.35	0.66	0.49	0.25	0.42	0.53	0.62	0.51	0.43	0.33	0.52	0.41	0.42	0.5	0.41	0.33	0.45
Be																	
Sc																	
V																	
Cr																	
Co																	
Ni	41	57	73	7	58	33	33	60	37	71	25	29	63	81	41	131	80
Cu	134	109	326	6	211	217	244	263	157	142	210	159	191	341	183	176	220
Zn	59	59	140	18	107	68	75	118	111	81	80	77	112	132	81	93	138
Ga																	

Note: Oxides are in weight percent. Elements in ppm; the Th data are the maximum possible values (except in Gujarat samples); Mg# = Mg/(Mg+Fe); *Fe_2O_3 calculated assuming 15% of total Fe as in ferric state

Table 1. *Contd...*

	Panna-Jabalpur-Seoni-Nagpur															
	CHF-1 flow	JD-1 dyke	JSD-1 dyke	JSD-4 dyke	JSD-6 dyke	JSD-7 dyke	JSD-10 dyke	JSD-11 dyke	JSD-14 dyke	397DY8586 dyke	NSF-1 flow	JSF-4 flow	JSF-7 flow	JSF-8 flow	JSF-13 flow	JSF-15 flow
SiO_2	47.89	48.03	47.21	50.15	50.17	48.4	50.77	49.09	47.9	47.28	48.27	49.53	47.42	48.9	47.84	47.65
TiO_2	2.49	1.33	1.37	1.1	2.25	1.82	1.37	2.29	2.02	0.93	2.58	3.29	3.12	1.81	2.91	2.91
Al_2O_3	13.11	15.69	14.38	13.61	14.32	15.08	13.98	13.53	13.38	15.58	13.01	112.25	13.33	13.81	13.01	12.64
Fe_2O_3	15.89	13.73	12.16	13.98	14.23	13.08	13.38	14.81	14.03	13.76	15.67	15.92	15.01	13.33	15.96	16.39
MnO	0.2	0.19	0.17	0.22	0.17	0.17	0.19	0.2	0.2	0.39	0.22	0.22	0.2	0.17	0.2	0.2
MgO	5.59	7.2	6.64	6.04	4.91	6.75	5.82	5.58	5.84	7.9	5.17	4.34	5.44	6.3	5.33	5.41
CaO	10.48	10.21	12.64	10.78	9.91	11.38	10.55	10.33	10.8	12.03	10.21	9.08	10.58	11.28	10.08	10.19
Na_2O	2.38	2.34	2.11	2.2	2.22	2.31	2.29	2.52	2.22	1.75	2.41	2.52	2.49	2.25	2.32	2.25
K_2O	0.24	0.78	0.15	0.25	0.65	0.25	0.63	0.43	0.14	0.15	0.29	0.72	0.17	0.11	0.19	0.17
P_2O_5	0.34	0.3	0.15	0.17	0.25	0.19	0.17	0.25	0.32	0.2	0.38	0.39	0.38	0.2	0.34	0.43
LOI			2.79	1.3	0.67	0.36	0.68	0.77			0.73	1.48	1.57	1.63	1.58	
Total	98.61	99.8	99.77	99.8	99.75	99.79	99.83	99.8	96.85	99.97	98.94	99.74	99.71	99.79	99.76	98.24
Fe_2O_3*	2.38	2.06	1.82	2.10	2.13	1.96	2.01	2.22	2.10	2.06	2.35	2.39	2.25	2.00	2.39	2.46
FeO*	12.15	10.50	9.30	10.69	10.88	10.00	10.23	11.33	10.73	10.52	11.99	12.18	11.48	10.20	12.21	12.54
Mg#	45.05	55.00	56.00	50.17	44.57	54.60	50.34	46.76	49.24	57.23	4347	38.85	45.79	52.42	43.77	43.48
Rb	15	21	8	18	19	10	22	17	8	5	13	17	12	9	6	8
Ba	57	230	55	103	188	62	144	93	52	8	77	211	91	56	121	90
Th	5	5	5	5	5	5	5	5	5	5	5	5	5	5	5	5
Nb	13	6	8	8	9	8	9	11	11	5	13	20	21	9	14	17
Ta																
Sr	205	216	193	101	250	205	129	200	197	111	231	217	237	208	216	213
Hf																
Zr	131	66	82	79	167	104	112	146	115	29	148	250	188	111	181	171
Y	35	23	22.51	30.16	31.65	24.64	33.1	31.43	30	22	35	45.17	36.15	26.72	36.74	36
La	12.41	12.27	8.33	9.61	20.88	9.32	14.07	13.39	12.11		14.26	26.04	18.59	10.72	17.53	16.8
Ce	35.86	30.41	17.49	20.12	44.14	20.8	28.18	29.06	31.02		34.68	55.03	41.61	24.26	38.91	47.38
Pr																
Nd	19.17	13.87	11.23	9.68	26.12	14.3	15.11	19.73	16.64		19.66	34.57	27.17	15.91	25.6	23.63
Sm	5.76	3.69	3.68	3.32	7.27	4.25	4.75	6.04	4.64		5.85	9.88	7.53	4.59	7.33	6.49
Eu	1.95	1.28	1.22	0.96	2.24	1.45	1.36	1.87	1.6		1.97	2.71	2.37	1.54	2.24	2.09
Gd	5.95	3.75	4.14	3.95	7.14	3.98	5.2	5.94	4.95		6.01	9.62	7.78	5.03	7.47	6.43
Tb	0															
Dy	5.54	3.53	4.05	4.78	6.53	4.49	5.81	5.99	4.67		5.5	8.97	7.23	4.83	7.18	6.09
Ho																
Er	3.04	2.11	1.89	2.78	2.82	1.87	3.06	2.66	2.48		2.84	4.09	2.89	2.14	3.22	3.26
Tm																
Yb	2.79	2.01	1.88	3.21	2.74	2.17	3.19	2.8	2.41		2.6	3.79	3.12	2.3	3.33	3.04
Lu	0.47	0.37	0.25	0.47	0.38	0.27	0.45	0.39	0.41		0.48	0.53	0.44	0.33	0.48	0.44
Be			1.29	1.29	1.6	1.2	1.29	1.6				1.79	1.7	1.2	1.7	
Sc			36.4	44.7	31.7	33.9	39.4	36.2				31.1	33.7	36.2	36.5	
V			348	376	352	346	369	408				462	476	378	445	
Cr			269	166	88	242	118	98				63	236	173	112	
Co			43	44	40	44	42	43				37	41	47	43	
Ni	84	94	102	72	68	99	66	30	78	132	75	58	112	92	75	65
Cu	270	59	117	143	144	152	167	183	216	40	255	232	248	144	233	308
Zn	113	96	85	107	105	91	89	111	102	170	116	129	124	97	122	124
Ga			15	14	18	16	16	17				23	24	19	20	

Note: Oxides are in weight percent. Elements in ppm; the Th data are the maximum possible values (except in Gujarat samples); Mg# = Mg/(Mg+Fe); *Fe_2O_3 calculated assuming 15% of total Fe as in ferric state

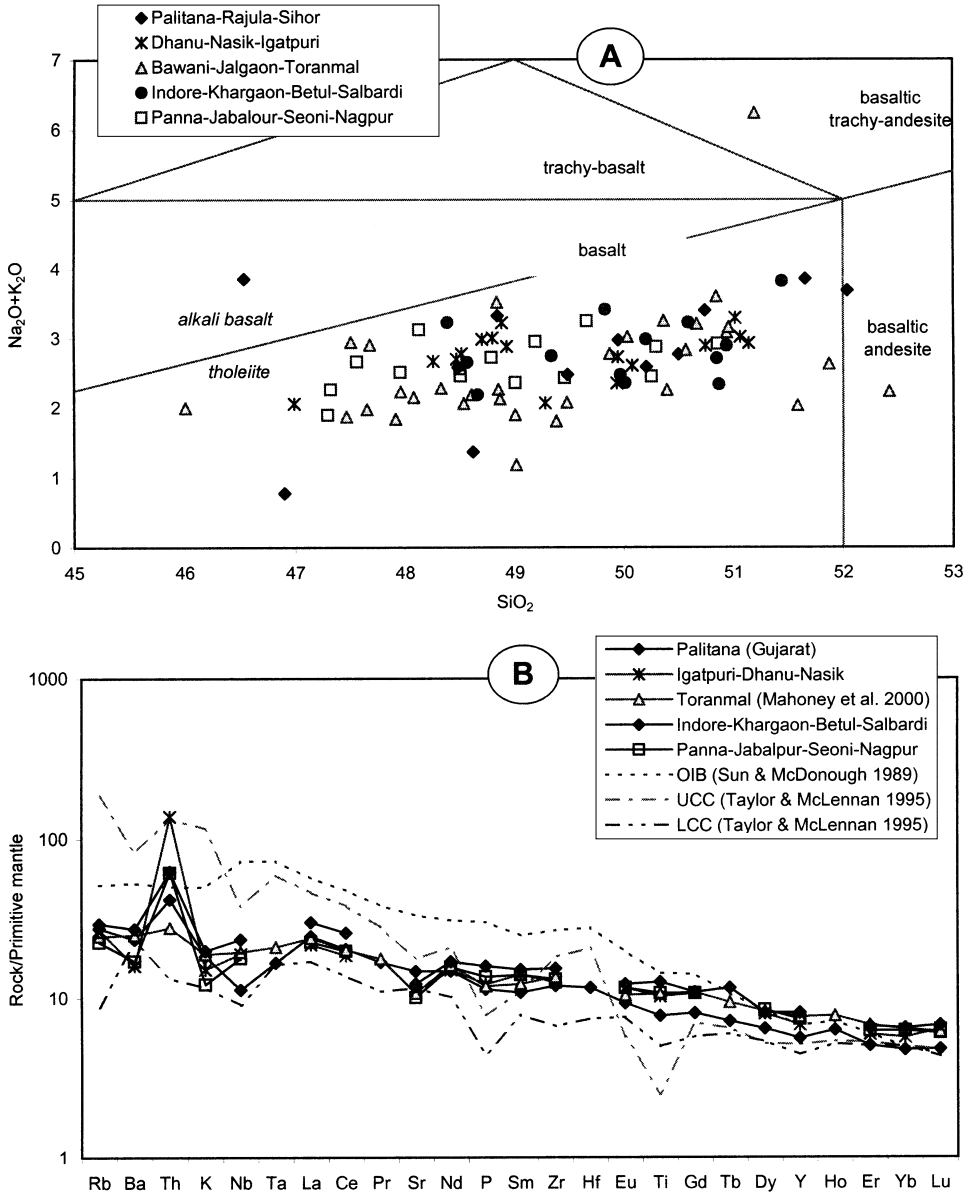

Fig.3. (**a**) SiO_2 wt % plotted against total alkali, Na_2O+K_2O wt %. The alkali basalt-tholeiite boundary is from Macdonald and Katsura (1964) and the other compositional boundaries are from Le Bas et al. (1986). (**b**) Primitive mantle-normalized (McDonough and Sun, 1995) incompatible element abundances of average basalts from the five areas of the Deccan province in this study compared with the abundances in oceanic island basalts (OIB) and upper and lower continental crust (UCC and LCC). In both diagrams, data for the Toranmal basalts (Mahoney et al. 2000) are included.

composition for the Palitana lavas. However, the incompatible element signatures all the Deccan samples in this study differ significantly from oceanic island basalts and show similarities with continental crust (Fig. 3b), which shows Nb-Ta and Ti troughs, high La/Nb ratios (1.2-1.8, Taylor and McLennan, 1995) and low Nb/Ta ratios (~12-13, Barth et al. 2000; Pfander et al. 2007). The incompatible element signatures of the Deccan tholeiites thus show evidences of crustal contamination.

The results of trace element modeling are plotted in Figs. 4, 5 and 6. The trace element contents of mantle partial melts for different fractions of melting are shown in Figs. 4a and 5a. The melting models indicate that the Zr content and Rb/Nb (i.e., approximately equal increase in Rb/Y and Nb/Y) are somewhat constant during low to moderate partial melting (1-20%) of mantle. However, Ba/Zr, Rb/Y and Nb/Y values are high for low degrees of melting. Figs. 4 and 5 show that much of the variation in

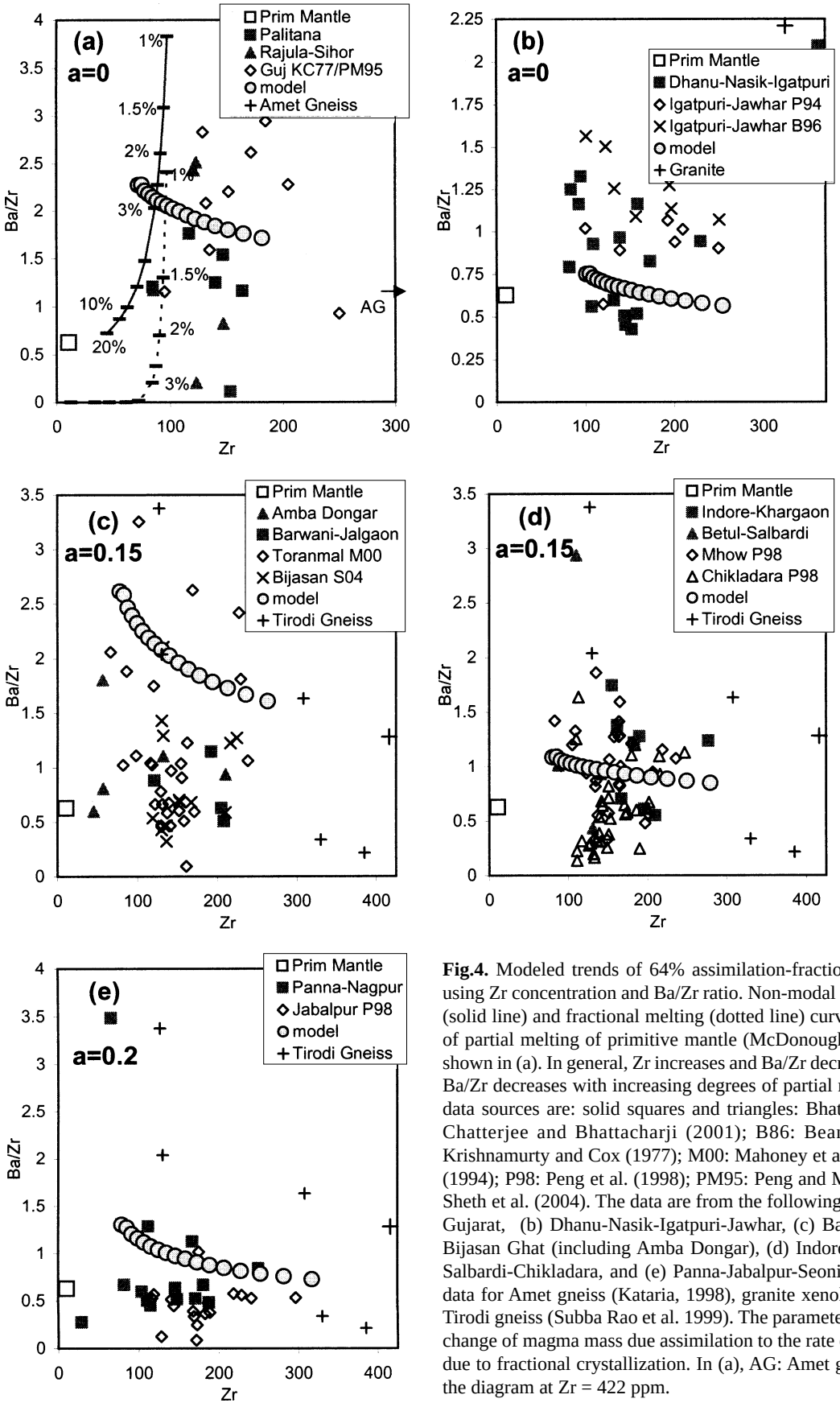

Fig.4. Modeled trends of 64% assimilation-fractional crystallization (AFC) using Zr concentration and Ba/Zr ratio. Non-modal equilibrium batch melting (solid line) and fractional melting (dotted line) curves at different percentage of partial melting of primitive mantle (McDonough and Sun, 1995) are also shown in (a). In general, Zr increases and Ba/Zr decreases with AFC, whereas, Ba/Zr decreases with increasing degrees of partial melting. The symbols and data sources are: solid squares and triangles: Bhattacharji et al. (1996) and Chatterjee and Bhattacharji (2001); B86: Beane et al. (1986); KC77: Krishnamurty and Cox (1977); M00: Mahoney et al. (2000); P94: Peng et al. (1994); P98: Peng et al. (1998); PM95: Peng and Mahoney (1995) and SO4: Sheth et al. (2004). The data are from the following areas: (a) Sihor-Palitana-Gujarat, (b) Dhanu-Nasik-Igatpuri-Jawhar, (c) Barwani-Jalgaon-Toranmal-Bijasan Ghat (including Amba Dongar), (d) Indore-Mhow-Khargaon-Betul-Salbardi-Chikladara, and (e) Panna-Jabalpur-Seoni-Nagpur. Also shown are data for Amet gneiss (Kataria, 1998), granite xenolith (Lightfoot, 1985) and Tirodi gneiss (Subba Rao et al. 1999). The parameter "a" is the ratio of rate of change of magma mass due assimilation to the rate of change of magma mass due to fractional crystallization. In (a), AG: Amet gneiss plots to the right of the diagram at Zr = 422 ppm.

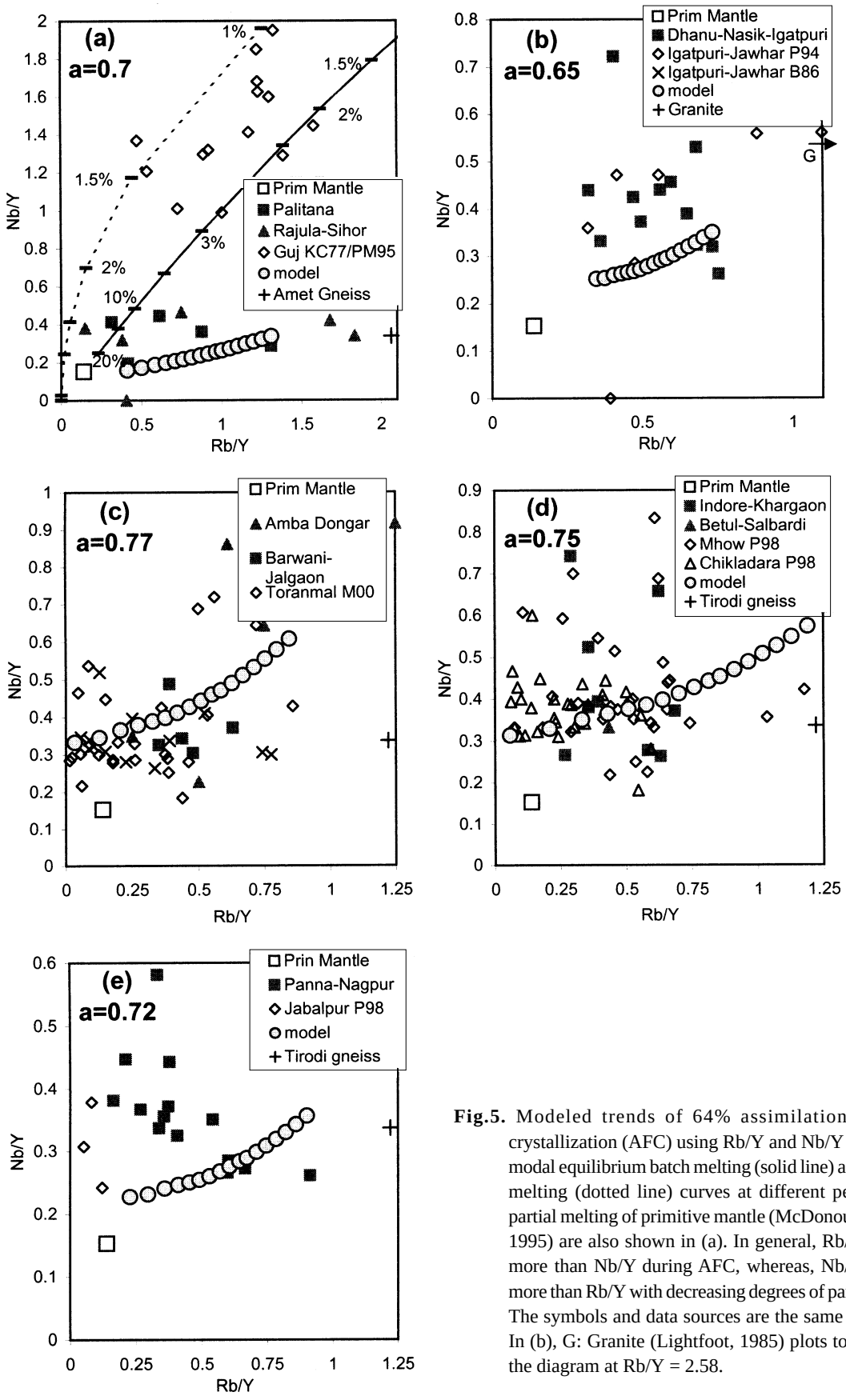

Fig.5. Modeled trends of 64% assimilation-fractional crystallization (AFC) using Rb/Y and Nb/Y ratios. Non-modal equilibrium batch melting (solid line) and fractional melting (dotted line) curves at different percentage of partial melting of primitive mantle (McDonough and Sun, 1995) are also shown in (a). In general, Rb/Y increases more than Nb/Y during AFC, whereas, Nb/Y increases more than Rb/Y with decreasing degrees of partial melting. The symbols and data sources are the same as in Fig. 4. In (b), G: Granite (Lightfoot, 1985) plots to the right of the diagram at Rb/Y = 2.58.

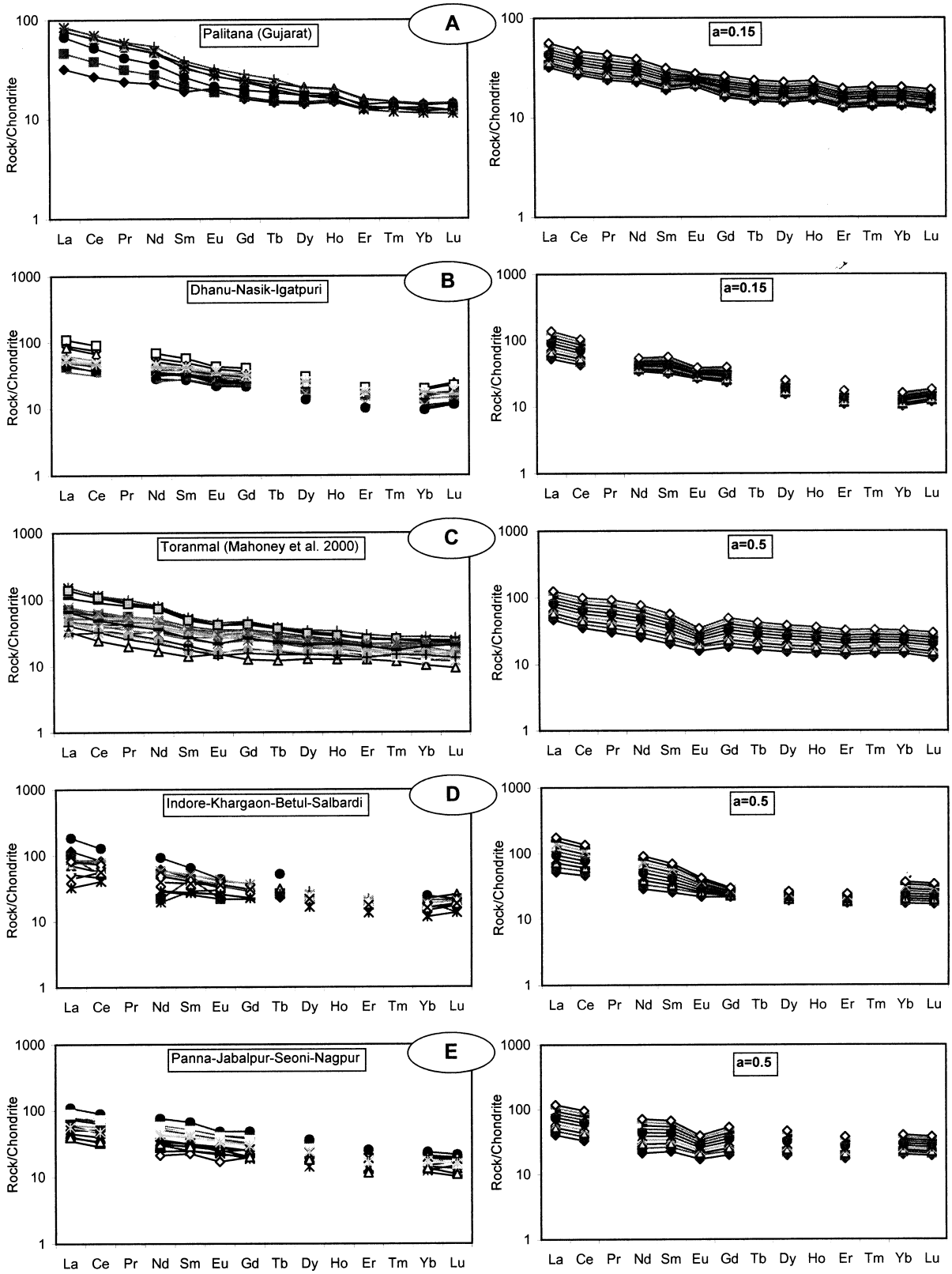

Fig.6. Chondrite normalized (McDonough and Sun, 1995) rare earth element abundances of basalts from the five areas of the Deccan province and modeled trends of 64% assimilation-fractional crystallization. The highest REE abundances are for the most fractionated (64%) compositions. In each area, the variation in the REE's corresponds to AFC fractionation of parental basalt roughly between 0 and 64%.

these ratios in the Deccan basalts can be attributed to low to moderate degrees of mantle melting. The Gujarat picrites and basalts (Krishnamurthy and Cox, 1977; Peng and Mahoney, 1995) are especially products of low degrees of partial melting of mantle (Figs. 4a and 5a).

The variations in Zr (Fig. 4) and Rb/Y (Fig. 5) can be explained by basaltic differentiation. In these calculations, the parental magmas may be considered as averages of different parental magmas generated by different degrees of partial melting of the mantle source. In general, fractional crystallization alone is sufficient to explain the range of Zr concentrations in the Gujarat and Igatpuri-Dhanu-Nasik areas (Figs. 4a,b). Fractional crystallization with moderate amounts of crustal assimilation (a = 0.15-0.2) are required to explain the range of Zr in the basalts from the Narmada-Tapti rift (Fig. 4c,d,e). To explain the Rb/Y ratios, however, high amounts of crustal assimilation (Fig. 5) are required. Nevertheless, crustal assimilation seems to be higher in the Narmada-Tapti rift area (a = 0.72-0.77) than in the Dhanu-Nasik-Igatpuri (a = 0.65) and Gujarat (a = 0.70) areas. The AFC modeling results for REE are compared with the REE abundances in each of the five areas in Fig. 6. The "a" values required to explain the REE variations are higher than those required in the Zr-based models but lower than in the Rb/Y-based models. However, the pattern of high crustal assimilation in the Narmada-Tapti rift area (a=0.5) and low crustal assimilation the Dhanu-Nasik-Igatpuri and Gujarat areas (a=0.15) is also discernable in the REE-based models.

In contrast, fractional crystallization with very high amounts of assimilant (a = 0.90-0.95) are required to explain the ranges of the $^{87}Sr/^{86}Sr$ and e_{Nd} values in all the different areas of the Deccan province (Fig. 7). In fact, the Igatpuri-Jawhar data are not reproduced even with an "a" value of 0.95 (Fig. 7b).

DISCUSSION

Isotope data from various studies (Fig. 7) provide incontrovertible evidence of crustal contamination in the Deccan basalts. However, the unreasonably high estimates of "a" values required in the AFC calculations involving Sr-Nd isotope data (Fig. 7) imply that the magma mass remained practically constant, a condition that could not have been possible. We also attempted to reproduce part of the Sr-Nd isotope data starting from the CS composition (Figs. 7a,c,d) to verify if the second stage of the two-stage model (Peng et al. 1994) involved AFC. The assimilant amounts required did not change significantly. Hence, the isotopic characteristics of the Deccan basalts must have been acquired before AFC of the parental magmas occurred (Cox and Hawkesworth, 1985) in shallow upper crustal magma chambers. Positive correlation between contamination and fractionation indices in some upper Deccan formations was explained by a "temperature controlled assimilation" mechanism that involves insulation of the walls of magma chambers and conduits with solidified basalt after the initial magma pulse preventing interaction of the differentiated magma and later magma batches with the wall rocks (Cox and Hawkesworth, 1984, 1985; Devey and Cox, 1987; Mahoney, 1988). Our calculations suggest that the largest changes in the isotopic ratios occur during the initial stages of 4-12% fractionation (Fig. 7). Thus, even small interactions with the wall rock might have altered the isotopic ratios of the parental magmas significantly.

Evidence of AFC-related crustal contamination was previously demonstrated in isolated parts of the Deccan province where silicic lavas were erupted (Sheth and Ray, 2002; Chatterjee and Bhattacharji, 2001) and where basaltic magma interacted with Maastrichtian Lameta beds and shale (Salil et al. 1997; Chandrasekharam et al. 2000). In this study, AFC modeling with Zr and REE indicate low to moderate amounts of crustal assimilation in the Gujarat and the western continental margin (Figs. 4, 6). The Rb/Y- and REE-based models require significant amounts of assimilant in the Narmada-Tapti area (Figs. 5, 6). Presence of multiple parental magmas may have affected these calculations. However, the high assimilant requirements in Rb/Y-based models may also be due to the relatively high compatibility of Rb in plagioclase. Large amounts of crust are required to compensate the decrease in Rb (in melt) due to plagioclase dominated fractional crystallization and increase the net abundance of Rb in the differentiated liquids. The greater incompatibility of Rb relative to Zr may also have facilitated incorporation of some Rb in the parental melts prior to basaltic differentiation. The Zr-based models thus provide better estimates of assimilant amounts.

In all the models (Figs. 4, 5 and 6), the estimated assimilant amounts are higher in areas away from the plume center at the western continental margin (Fig. 1, Bhattacharji et al. 1996). The Zr-based models indicate that there was no crustal assimilation near the plume center and the Zr, REE and Rb/Y-based models indicate that the amount of assimilant increased away from the plume center in the Narmada-Tapti rift. This trend may be a consequence of changes in physical and chemical conditions and magma dynamics from the plume center to the edge of the province. Near the plume center, the initial batches of magma were probably contaminated as they interacted with the fertile wall rock. However, the more voluminous later batches were less affected because of isolation of the wall rocks by

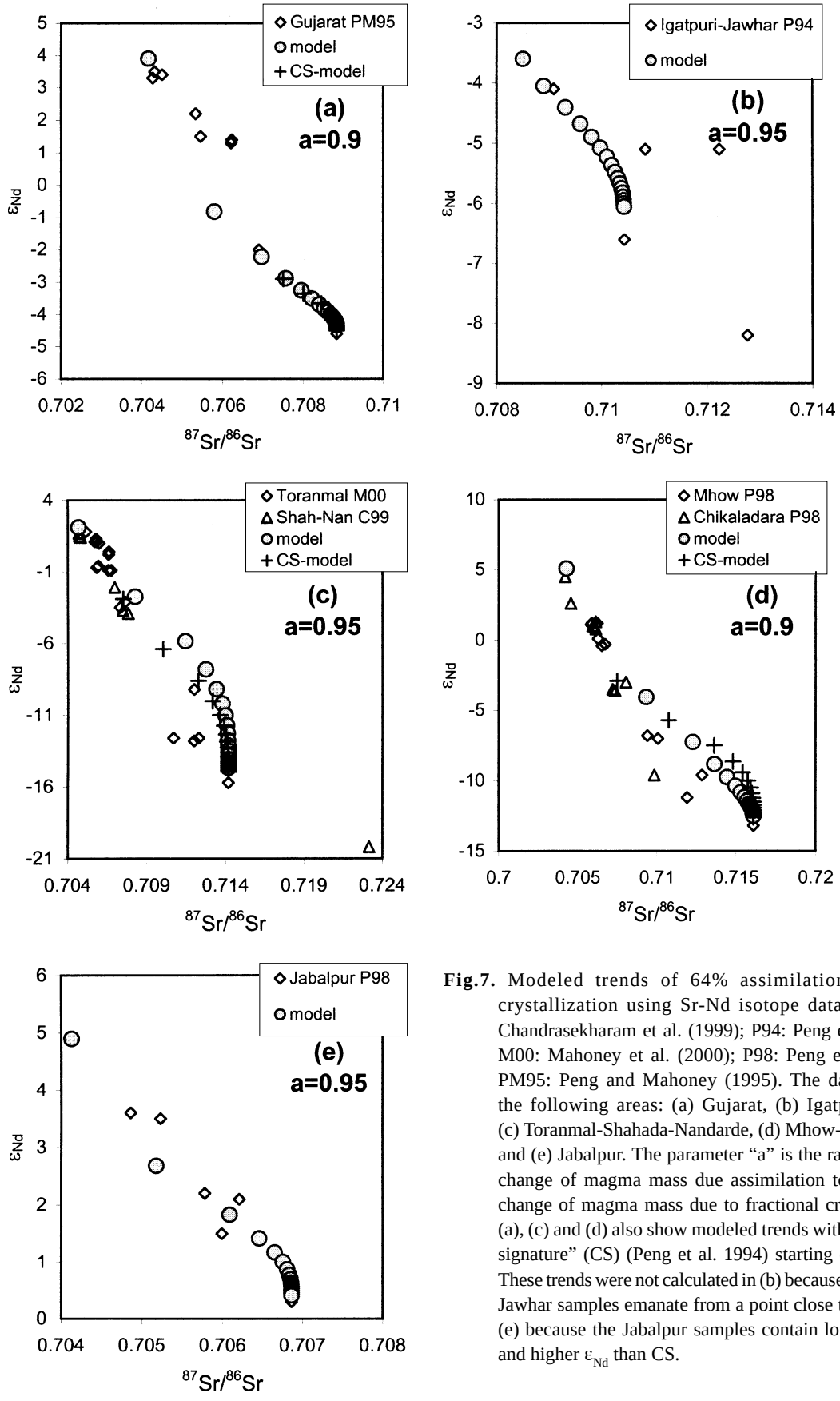

Fig.7. Modeled trends of 64% assimilation-fractional crystallization using Sr-Nd isotope data from C99: Chandrasekharam et al. (1999); P94: Peng et al. (1994); M00: Mahoney et al. (2000); P98: Peng et al. (1998); PM95: Peng and Mahoney (1995). The data are from the following areas: (a) Gujarat, (b) Igatpuri-Jawhar, (c) Toranmal-Shahada-Nandarde, (d) Mhow-Chikaladara, and (e) Jabalpur. The parameter "a" is the ratio of rate of change of magma mass due assimilation to the rate of change of magma mass due to fractional crystallization. (a), (c) and (d) also show modeled trends with a "common signature" (CS) (Peng et al. 1994) starting composition. These trends were not calculated in (b) because the Igatpuri-Jawhar samples emanate from a point close to CS, and in (e) because the Jabalpur samples contain lower $^{87}Sr/^{86}Sr$ and higher ε_{Nd} than CS.

previously crystallized material or because the wall rocks had become too refractory to melt and supply the trace elements under consideration. In the Narmada-Tapti rift region, the northward movement of the Indian plate and north-south extension along the rift resulted in the formation of several shallow crustal magma chambers (Kaila et al. 1985; Kaila, 1988; Kaila and Krishna, 1992; Bhattacharji et al. 2004). Mechanical processes inside the magma chambers such as wall rock scouring and stoping were aided by crustal extension. As a result, the magma chambers were enlarged creating space for fresh magma to enter the magma chambers. Enlargement of the magma chambers also exposed more of the fertile wall rock to the fresh, hot magma. Convective mixing of the fresh, hot magma and the previous magma in the enlarged magma chambers enabled assimilation of fertile wall rock over a longer period. Thus, increase in the magma chamber size and heat from fresh magma resulted in longer and greater magma-wall rock interaction and crustal assimilation in the shallow crustal magma chambers in the Narmada-Tapti rift region.

There are many possible upper crustal contaminants for the Deccan basalts. These include granitic xenolith from the west coast (Lightfoot, 1985), Bundelkhand, Tirodi and Bastar gneisses (Rahman and Zainuddin, 1993; Ramachandra and Roy, 2001; Subba Rao et al. 1999; Sarkar et al. 1993) near Jabalpur and Indore, and the Amet gneisses of Rajasthan (Kataria, 1998). Trace element data for the possible contaminants are plotted in Figs. 4 and 5. With few exceptions, these data plot on the same trend as that defined by the AFC models strongly indicating that these granites and gneisses have indeed contaminated the Deccan basalts. Five out of seven samples of Tirodi gneiss (Subba Rao et al. 1999) show the same range of Zr (Figs. 4c,d,e), indicating that Tirodi gneiss may have contaminated the Deccan basalts in the Narmada-Tapti rift area.

CONCLUSION

Our modelling indicates that although variations in Ba/Zr, Rb/Y and Nb/Y ratios of the Deccan basalts may be explained by low to moderate degrees of partial melting of mantle, significant amounts of crustal assimilation by the Deccan magmas are required to explain the variations in Zr, REE and Rb/Nb in basalts away from the plume center. In general, the Zr contents of the basalts of the Dhanu-Nasik-Igatpuri area near the plume center can be explained by only fractional crystallization without the involvement of crust. Available Sr-Nd isotope data require very high and unreasonable amounts of assimilant in the Gujarat, the Narmada-Tapti rift and the western continental rift regions of the Deccan province implying that the parental magmas may have acquired their isotopic characteristics before AFC happened in shallow magma chambers. The greater crustal assimilation in the Narmada-Tapti rift region may be related to longer and greater magma-wall rock interaction in shallow crustal magma chambers due to crustal extension-related enlargement of the magma chambers, recharge with fresh, hot magma and convective mixing.

Acknowledgements: We acknowledge the help of the French National Laboratory, Nancy, France in obtaining high quality chemical analyses of the Deccan basalts. This study was supported by an international grant from the National Science Foundation to S.B. We greatly appreciate the constructive reviews and the comments of the reviewers.

References

ALLEGRE, C.J., BIRCK J.L., CAPMAS, F. and COURTILLOT V. (1999) Age of the Deccan traps using ^{187}Re-^{187}Os systematics. Earth Planet. Sci. Lett., v.170, pp.197-204.

BAKSI, A.K. (1994) Geochronological studies on whole-rock basalts, Deccan Traps, India: evaluation of the timing of volcanism relative to the K-T boundary. Earth Planet. Sci. Lett. v.121, pp.43-56.

BARTH, M.G., MCDONOUGH, W.M. and RUDNICK, R.L. (2000) Tracking the budget of Nb and Ta in the continental crust. Chemical Geol., v.165, pp.197-213.

BASU, A.R., RENNE, P.R., DASGUPTA, D.K., TEICHMAN, F. and POREDA, R.J. (1993) Early and late igneous pulses and a high-^{3}He plume origin for the Deccan flood basalts. Science, v.261, pp.902-906.

BEANE, J.E., TURNER, C.A., HOOPER, P.R., SUBBARAO, K.V. and WALSH, J.N. (1986) Stratigraphy, composition and form of the Deccan basalts, Western Ghats, India. Bull. Volcanol., v.48, pp.61-83.

BEDARD, J. (2001) Parental magmas of the Nain Plutonic Suite anorthosites and mafic cumulates: a trace element modelling approach. Contrib. Mineral. Petrol., v.141, pp.747-771.

BHATTACHARJI, S. and KOIDE, H. (1987) Theoretical and experimental studies of mantle upwelling, penetrative magmatism, and development of rifts in continental and oceanic crusts. Tectonophysics, v.143, pp.13-30.

BHATTACHARJI, S., CHATTERJEE, N., WAMPLER, J.M., NAYAK, P.N. and DESHMUKH, S.S. (1996) Indian intraplate and continental margin rifting, lithospheric extension, and mantle upwelling in Deccan flood basalt volcanism near the K/T boundary: evidence from mafic dike swarms. Jour. Geol., v.104, pp.379-398.

BHATTACHARJI, S., SHARMA, R. and CHATTERJEE, N. (2004) Two-

and three-dimensional gravity modeling along western continental margin and intraplate Narmada-Tapti rifts: Its relevance to Deccan flood basalt volcanism. Proc. Indian Acad. Sci. (Earth Planet. Sci.), v.114/4, pp.771-784.

BONDRE, N.R., HART, W.K. and SHETH, H.C. (2006) Geology and Geochemistry of the Sangamner Mafic Dike Swarm, Western Deccan Volcanic Province, India: Implications for Regional Stratigraphy. Jour. Geol., v.114, pp.155-170.

BOSE, M.K. (1980) Magmatically defined tectonic framework of the Deccan volcanics province. N. Miner. Jb., v.8, pp.373-384.

BURKE, K.C. and DEWEY, J.F. (1973) Plume generated triple junctions: key indicators in applying plate tectonics to old rocks. Jour. Geol., v.81, pp.403-433.

CAMPBELL, I.H. and GRIFFITHS, R.W. (1990) Implications of mantle plume structure for the evolution of flood basalts. Earth Planet. Sci. Lett., v.99, pp.79-93.

CHANDRASEKHARAM, D., MAHONEY, J.J., SHETH, H.C. and DUNCAN, R.A. (1999) Elemental and Nd-Sr-Pb isotope geochemistry of flows and dikes from the Tapi rift, Deccan flood basalt province, India. Jour. Volcanol. Geotherm. Res., v.93, pp.111-123.

CHANDRASEKHARAM, D., VASELLI, O., SHETH, H.C. and KESHAV, S., 2000. Petrogenetic significance of ferro-enstatite orthopyroxene in basaltic dikes from the Tapi rift. Deccan flood basalt province, India. Earth Planet. Sci. Lett., v.179, pp.469-476.

CHATTERJEE, N. and BHATTACHARJI, S. (2001) Origin of felsic and basaltic dikes and flows in the Rajula–Palitana–Sihor area of the Deccan Traps. India: a geochemical and geochronological study. Internat. Geol. Rev., v.43, pp.1094-1116.

COURTILLOT, V., BESSE, J., VANDAMME, D., MONTIGNY, R., JAEGER, J.J. and CAPPETTA, H. (1986) Deccan flood basalts at the Cretaceous/ Tertiary boundary? Earth Planet. Sci. Lett., v.80, pp.361-374.

COURTILLOT, V.E., FERAUD, G., MALUSKI, H., VANDAMNE, D., MOREAU, M.G. and BESSE, J. (1988) Deccan flood basalts and the Cretaceous-Tertiary boundary. Nature, v.333, pp.843-846.

COURTILLOT, V.E., JAUPART, C., MANIGHETTI, I., TAPPONNIER, P. and BESSE, J. (1999) On causal links between flood basalts and continental breakup. Earth Planet. Sci. Lett., v.166, pp.177-195.

COX, K.G. (1983) Deccan Traps and the Karoo: stratigraphic implications of possible hot spot origins. IAVCEI programme and abstracts of XXIII IUGG General Assembly, Hamburg, p.96.

COX, K.G. and HAWKESWORTH, C.J. (1984) Relative contribution of crust and mantle to flood basalt magmatism, Mahabaleshwar area, Deccan Traps. Philos. Trans. R. Soc. London, v.A310, pp.627-641.

COX, K.G. and HAWKESWORTH, C.J., 1985. Geochemical stratigraphy of the Deccan Traps at Mahabaleshwar, Western Ghats, India, with implication for open system processes. Jour. Petrol., v.26, pp.355-387.

DEPAOLO, D.J. (1981) Trace element and isotopic effects of combined wallrock assimilation and fractional crystallization. Earth Planet. Sci. Lett., v.53, pp.189-202.

DEVEY, C.W. and COX, K.G. (1987) Relationships between crustal contamination and crystallisation in continental flood basalt magmas with special reference to the Deccan Traps of the Western Ghats, India. Earth Planet. Sci. Lett., v.84, pp.59-68.

DEVEY, C.W. and LIGHTFOOT, P.C. (1986) Volcanological and tectonic control of stratigraphy and structure in the western Deccan Traps. Bull. Volcanol., v.48, pp.195-207.

DUNCAN, R.A. and PYLE, D.G. (1988) Rapid eruption of the Deccan flood basalts at the Cretaceous/Tertiary boundary. Nature, v.333, pp.841-843.

DUNCAN, R.A. and RICHARDS, M.A. (1991) Hot spots, mantle plumes, flood basalts, and true polar wander. Rev. Geophys., v.29, pp.31-50.

HOOPER, P.R. (1994) Sources of continental flood basalts: the lithospheric component. *In:* K.V. Subbarao, (Ed.), Volcanism. New Delhi, Wiley Eastern, pp.29-53.

HUPPERT, H.E. and SPARKS, R.S.J. (1985) Cooling and contamination of mafic and ultramafic magmas during ascent through the continental crust. Earth Planet. Sci. Lett., v.74, pp.372-386.

KAILA, K.L. (1988) Mapping the thickness of Deccan trap flows in India from DSS studies and inferences about a hidden Mesozoic basin in Narmada-Tapti region. *In:* K.V. Subbarao, (Ed.), Deccan Flood Basalts. Mem. Geol. Soc. India, No.10, pp.96-116.

KAILA, K.L. and KRISHNA, V.G. (1992) Deep seismic sounding studies in India and major discoveries. Curr. Sci., v.62, pp.117-154.

KAILA, K.L., REDDY, P.R., DIXIT, M.M. and KOTESWARA RAO, P. (1985) Crustal structure across the Narmada-Son lineament, Central India from deep seismic soundings. Jour. Geol. Soc. India, v.26, pp.465-480.

KATARIA, P. (1998) Petromineralogy and geochemistry of the Precambrian shear zone rocks of Amet, Rajasthan. *In:* B.S. Paliwal (Ed.), "The Indian Precambrian". Jodhpur, India. Scientific Publishers, pp.263-271.

KRISHNAMURTHY, P. and COX, K.G. (1977) Picritic basalts and related lavas from the Deccan Traps of western India. Contrib. Mineral. Petrol., v.62, pp.53-75.

LE BAS, M.J., LE MAITRE, R.W., STRECKEISEN, A. and ZANETTIN, B. (1986) A chemical classification of volcanic rocks based on the total alkali-silica diagram. Jour. Petrol., v.27, pp.745-750.

LIGHTFOOT, P.C. (1985) Isotope and trace element geochemistry of the South Deccan lavas, India. Unpubl. Ph.D. thesis, The Open University, 589p.

LIGHTFOOT, P.C. and HAWKESWORTH, C.J. (1988) Origin of Deccan Trap lavas: evidence from combined trace element and Sr-, Nd- and Pb- isotope data. Earth Planet. Sci. Lett., v.91, pp.89-104.

LIGHTFOOT, P.C., HAWKESWORTH, C.J., DEVEY, C.W., ROGERS, N.W. and VAN CALSTEREN, P.W.C. (1990) Source and differentiation of Deccan Trap lavas: implications of geochemical and mineral chemical variations. Jour. Petrol., v.31, pp.1165-1200.

MACDONALD, G.A. and KATSURA, T. (1964) Chemical composition of Hawaiian lavas. Jour. Petrol., v.5, pp.82-133.

MAHONEY, J.J. (1988) Deccan Traps. *In:* J.D. Macdougall, (Ed.), Flood Basalts. Kluwer, Dordrecht, pp.151-194.

MAHONEY, J.J., MACDOUGALL, J.D., LUGMAIR, G.W., MURALI, A.V. and GOPALAN, K. (1982) Origin of the Deccan Traps flows at Mahabaleshwar as inferred from Nd and Sr isotope and chemical evidence. Earth Planet. Sci. Lett., v.60, pp.47-60.

MAHONEY, J.J., MACDOUGALL, J.J., LUGMAIR, J.D., GOPALAN, G.W. and KRISHNAMURTHY, K. (1985) Origin of contemporaneous tholeiitic and K-rich alkalic lavas: a case study from the

northern Deccan Plateau, India. Earth Planet. Sci. Lett., v.73, pp.39-53.

MAHONEY, J.J., SHETH, H.C., CHANDRASEKHARAM, D. and PENG, Z.X. (2000) Geochemistry of flood basalts of the Toranmal section, northern Deccan Traps, India: implications for regional Deccan stratigraphy. Jour. Petrol., v.41, pp.1099-1120.

MCDONOUGH, W.F. and SUN, S.S. (1995) The composition of the Earth. *In:* W.F. McDonough, N.T. Arndt and S. Shirey (Eds.), Chemical Evolution of the Mantle. Chem. Geol., v.120, pp.223-253.

MELLUSO, L., BARBIERI, M. and BECCALUVA, L. (2004) Chemical evolution, petrogenesis, and regional chemical correlations of the flood basalt sequence in the central Deccan Traps, India. *In:* K. Pande and H.C. Sheth (Eds.), Magmatism in India Through Time. Proc. Indian Acad. Sci., Earth Planet. Sci., v.113, pp.587-603.

MELLUSO, L., MAHONEY, J.J. and DALLAI, L. (2006) Mantle sources and crustal input as recorded in high-Mg Deccan Traps basalts of Gujarat (India). Lithos, doi:10.1016/j.lithos.2005.12.007

MITCHELL, C. and Widdowson, M. (1991) A geological map of the southern Deccan Traps, Indian and its structural implications. Jour. Geol. Soc. London, v.148, pp.495-505.

MORGAN, W.J. (1972) Deep mantle convection plumes and plate tectonics. Bull. Amer. Assoc. Petrol. Geologists, v.56(1), pp.203-213.

PENG, Z.X. and MAHONEY, J.J. (1995) Drillhole lavas in the Deccan Traps and the evolution of the Réunion plume. Earth Planet. Sci. Lett., v.134, pp.169-185.

PENG, Z.X., MAHONEY, J.J., HOOPER, P.R., HARRIS, C. and BEANE, J.E. (1994) A role for lower continental crust in flood basalt genesis? Isotopic and incompatible element study of the lower six formations of the Western Deccan Traps. Geochim. Cosmochim. Acta, v.58, pp.267-288.

PENG, Z.X., MAHONEY, J.J., HOOPER, P.R., MACDOUGALL, J.D. and KRISHNAMURTHY, P. (1998) Basalts of the northeastern Deccan Traps, India: isotopic and elemental geochemistry and relation to southwestern Deccan stratigraphy. Jour. Geophys. Res., v.103, pp.29843-29865.

PFÄNDER, J.A., MÜNKER, C., STRACKE, A. and MEZGER, K. (2007) Nb/Ta and Zr/Hf in ocean island basalts - Implications for crust-mantle differentiation and the fate of Niobium. Earth Planet. Sci. Lett., v.254, pp.158-172.

PRESNALL, D.C. (1969) The geometrical analysis of partial fusion. American Jour. Sci., v.267, pp.1178-1194.

RAHMAN, A. and ZAINUDDIN, S.M. (1993) Bundelkhand granites: an example of collision-related Precambrian magmatism and its relevance to the evolution of the Central Indian shield. Jour. Geol., v.101, pp.413-419.

RAMACHANDRA, H.M. and ROY, A. (2001) Evolution of the Bhandara-Balaghat granulite belt along the southern margin of the Sausar Mobile Belt of central India. Proc. Indian Acad. Sci. (Earth Planet. Sci.), v.110/4, pp.351-368.

RICHARDS, M.A., DUNCAN, R.A. and COURTILLOT, V.E. (1989a) Flood basalts and hotspot tracks: Plume heads and tails. Science, v.246, pp.103-107.

RICHARDS, M.A., DUNCAN, R.A. and COURTILLOT, V.E. (1989b) Flood basalt volcanism during the past 250 million years. Science, v.241, pp.663-668.

SAHA, A., BASU, A.R., BARLING, J., ANBAR, A.D. and HOOPER, P.R. (2001) Hf-Nd isotopic correlation in the Deccan flood basalt province. Eos. Trans. AGU, 82(47), Fall Meet. Suppl., Abstract V52-B05.

SARKAR, G., CORFU, F., PAUL, D.K., MCNAUGHTON, N.J., GUPTA, S.N. and BISHUI, P.K. (1993) Early Archean crust in Bastar Craton, Central India – a geochemical and isotopic study. Precambrian Res., v.62, pp.127-137.

SALIL, M.S., SHRIVASTAVA J.P. and PATTANAYAK, S.K. (1997) Similarities in the mineralogical and geochemical attributes of detrital clays of Maastrichtian Lameta Beds and weathered Deccan basalt, Central India. Chemical Geol., v.136, pp.25-32.

SANO, T., FUJII, T., DESHMUKH, S.S., FUKUOKA, T. and ARAMAKI, S. (2001) Differentiation processes of Deccan Trap basalts: contribution from geochemistry and experimental petrology. Jour. Petrol., v.42, pp.2175-2195.

SHAW, D.M., 1970. Trace element fractionation during anatexis. Geochim. Cosmochim. Acta, v.34(2), pp.237-243.

SHETH, H.C. and RAY, J.S. (2002) Rb/Sr-$^{87}Sr/^{86}Sr$ variations in Bombay trachytes and rhyolites (Deccan Traps): Rb-Sr Isochron, or AFC Process? Internat. Geol. Rev., v.44, pp.624-638.

SHETH, H.C., MAHONEY, J.J. and CHANDRASEKHARAM, D. (2004) Geochemical stratigraphy of Deccan flood basalts of the Bijasan Ghat section, Satpura Range, India. Jour. Asian Earth Sci., v.23, pp.127-139.

SUBBARAO, K.V. and HOOPER, P.R. (1988) Reconnaissance map of theDeccan Basalt Group in the Western Ghats, India. *In:* K.V. Subbarao (Ed.), Deccan Flood Basalts. Mem. Geol. Soc. India, No.10, 393p.

SUBBA RAO, M.V., NARAYANA, B.L., DIVAKARA RAO V. and Reddy, G.L.N. (1999) Petrogenesis of the protolith for the Tirodi gneiss by A-type granite magmatism: the geochemical evidence. Current Sci., v.76, pp.1258-1264.

SUN, S.-S. and MCDONOUGH, W.F. (1989) Chemical and isotopic systematics of oceanic basalts: implications for mantle compostion and processes. *In:* A.D. Saunders and D.J. Norry (Eds.), "Magmatisms in the ocean basins". Geol. Soc. Spec. Publ., no.42, pp.313-345.

TAYLOR, S.R. and MCLENNAN, S.M. (1995) The geochemical evolution of the continental crust. Reviews in Geophysics, v.33, pp.241-265.

VENKATESAN, T.R., PANDE, K. and GOPALAN, K. (1993) Did Deccan volcanism pre-date the Cretaceous/Tertiary transition? Earth Planet. Sci. Lett., v.119, pp.181-189.

VIJAYA KUMAR, K. (2006) Mantle melting models: an overview. Deep Continental Studies in India. CSIR Newsletter, v.16, pp.2-10.

WHITE, R.S. and MCKENZIE, D. (1989) Magmatism at rift zones: the generation of volcanic continental margins and flood basalts. Jour. Geophys. Res., v. 94, pp.7685-7729.

(Received: 6 March 2007; Revised form accepted: 13 June 2007)